Possible production of neutron-rich No isotopes

Myeong-Hwan Mun [1], Kyujin Kwak,[2,*] G. G. Adamian [3] and N. V. Antonenko[3,4]
[1]Korea Institute of Science and Technology Information, Daejeon 34141, Korea
[2]Ulsan National Institute of Science and Technology, Ulsan 44919, Korea
[3]Joint Institute for Nuclear Research, 141980 Dubna, Russia
[4]Tomsk Polytechnic University, 634050 Tomsk, Russia

(Received 18 September 2019; accepted 12 March 2020; published 6 April 2020)

We investigate possible production of neutron-rich isotopes of nobelium. We calculate the production cross sections of $^{261-266}$No in the multinucleon transfer reactions of the same projectiles (^{36}S, ^{40}Ar, ^{48}Ca, and ^{50}Ti) and targets (^{254}Es and $^{248-251}$Cf) that were used in the previous study for the possible production of neutron-rich isotopes of Md. We find that the production cross sections of neutron-rich No isotopes are about an order of magnitude smaller than those for neutron-rich Md isotopes. By combining the results for the production of neutron-rich No and Md isotopes, we suggest simple expressions which can trace the isotopic trends of the production cross sections of heavy neutron-rich isotopes. The logarithm of the production cross section is proportional to isospin of projectile or target and the Q value.

DOI: 10.1103/PhysRevC.101.044602

I. INTRODUCTION

New isotopes of transfermium nuclei can be produced in either transfer-type or complete fusion reactions. Because possible sets of projectiles and targets are limited for complete fusion reactions to produce isotopes of heaviest nuclei, the transfer-type reactions are considered as the only way to extend the current nuclear chart by producing a number of new isotopes of heaviest nuclei. In particular, the multinucleon transfer reactions have been known to be effective for producing exotic nuclei for many years (see Refs. [1–26] for the applications of the multinucleon transfer reactions). As proven in Refs. [18,21,22,24,25], the transfer products accompany the complete fusion reactions. References [27–31] suggested that isotopes in the vicinity of the neutron dripline could be produced in the transfer reactions at incident energies close to the Coulomb barrier. Models in Refs. [29,32–35] predict the optimal projectile-target combinations as well as bombarding energies by estimating the production cross sections. Because the production cross sections of some neutron-rich isotopes are expected to be very small, theoretical estimates must be performed before the experiments.

In our previous work [36], we used the model of Refs. [34,35] and investigated possible production of neutron-rich isotopes of Md in multinucleon transfer reactions with Es and Cf as targets. We found that the reactions with the ^{36}S and ^{48}Ca beams have the largest production cross sections of unknown, i.e., experimentally unidentified yet, isotopes of Md. In the present paper, we extend our previous calculations [36] in order to study possible production of neutron-rich No isotopes in the same reactions that occur with projectiles of ^{36}S, ^{40}Ar, ^{48}Ca, and ^{50}Ti and targets of ^{254}Es and $^{248-251}$Cf. By combining the previous and current results, we suggest simple expressions that may reveal general trends in the production cross sections of neutron-rich isotopes of heaviest nuclei in the transfer reactions. Our paper is based on the assumption of statistical quasiequilibrium in mass (charge) asymmetry coordinate of the dinuclear system (DNS) formed in the entrance channel of a reaction. In comparison with Refs. [37–43], we consider the multinucleon transfer process at small angular momenta resulting in larger timescales. Because we are interested in the production of neutron-rich transfermium nuclei, the angular momentum injected in them has to be rather low to avoid fission. So, the partial waves up to 30 are taken into account in the calculations. The dynamical consideration with the master equation is certainly required if the product of charge numbers of projectile and target nuclei exceed 2500. Note that the method used cannot be applied to describe a few-nucleon transfer occurring at peripheral collisions during the short interaction time. For this purpose, the dynamical consideration based on either master or Langevin equations is suitable. The semimicroscopical models, e.g., GRAZING [44–46], are also suitable to describe the transfer of a few nucleons. Recent development in the quantum diffusion description of the multinucleon transfer reactions are based on the stochastic mean-field approach [47,48]. Although these calculations are time consuming, one can find the first and second moments of charge and mass distributions and estimate the isotopic yields assuming their Gaussian shapes.

This paper is organized as follows. In Sec. II, we briefly review the method of calculation. The calculated results for the production cross sections of neutron-rich isotopes of No are presented in Sec. III. In the same section, we discuss the general trends in the production cross sections of neutron-rich isotopes of Md and No in the transfer reactions. A summary is in Sec. IV.

*kkwak@unist.ac.kr

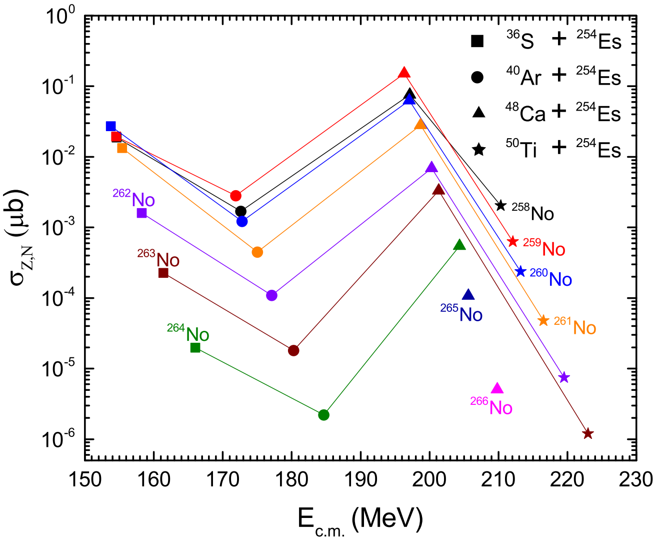

FIG. 1. The production cross sections of neutron-rich isotopes $^{258-266}$No calculated in the $0n$ evaporation channel as a function of incident energy $E_{\mathrm{c.m.}}$. Following multinucleon transfer, reactions are calculated: ^{36}S + ^{254}Es (squares), ^{40}Ar + ^{254}Es (circles), ^{48}Ca + ^{254}Es (triangles), and ^{50}Ti + ^{254}Es (stars). Lines with the same colors are drawn to trace the results of the same isotope of No.

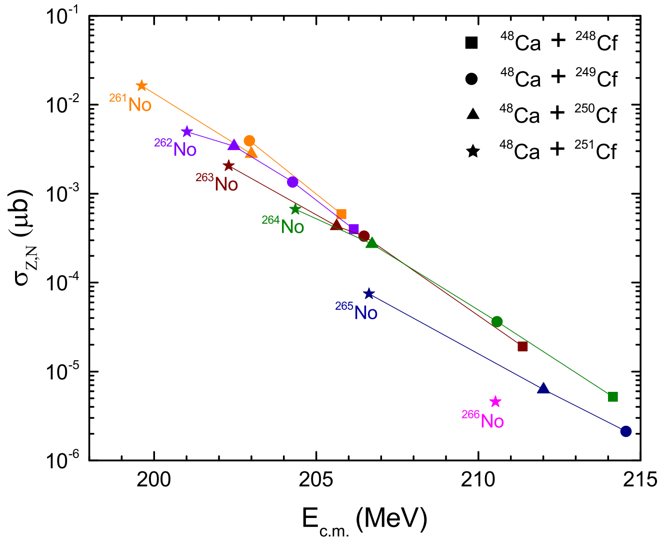

FIG. 3. The production cross sections of neutron-rich isotopes $^{261-266}$No calculated in the $0n$ evaporation channel as a function of incident energy $E_{\mathrm{c.m.}}$. Following multinucleon transfer, reactions are calculated: ^{48}Ca + ^{248}Cf (squares), ^{48}Ca + ^{249}Cf (circles), ^{48}Ca + ^{250}Cf (triangles), and ^{48}Ca + ^{251}Cf (stars). Lines with the same colors are drawn to trace the results for the same isotope of No.

II. METHOD OF CALCULATION

The nucleon transfer is naturally related to mass and charge asymmetry coordinates in the description of two interacting nuclei. For the calculation of the production cross sections of neutron-rich isotopes of No in the transfer reactions, we use the DNS model which can handle the multinucleon transfer in two interacting nuclei. In the DNS model, the interaction of two nuclei including nucleon transfer is described as follows. First, two nuclei encounter each other and lose their kinetic energy and angular momentum of the relative motion. After this dissipation of kinetic energy and angular momentum, the entrance channel DNS forms and contains the nucleus $(Z^{(i)}, N^{(i)})$ with charge number $Z^{(i)}$ and neutron number $N^{(i)}$. The DNS model uses three collective degrees of freedom, the mass and charge asymmetry coordinates defined through the charge Z and neutron N numbers of one DNS nucleus and the relative distance R between the centers of two interacting nuclei. In the calculation of the DNS potential energy, the nuclei are at touching distance $R = R_m$ which is a function of Z, N, and the deformations of nuclei. The entrance channel DNS evolves further through the nucleon drift and nucleon

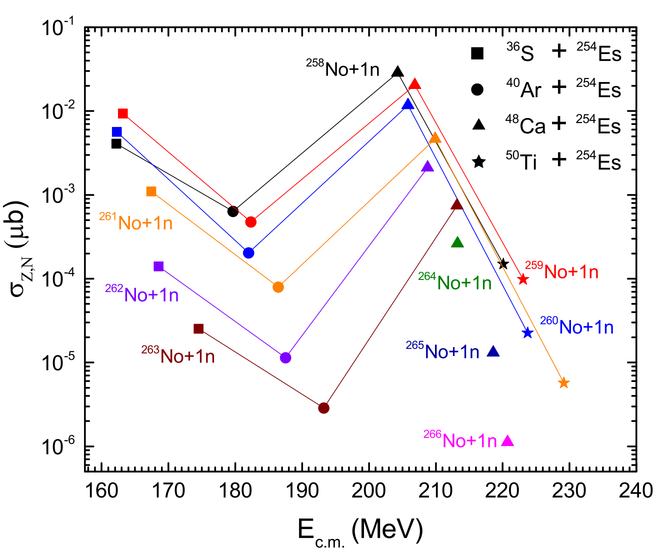

FIG. 2. The same as in Fig. 1 but in the $1n$ evaporation channel.

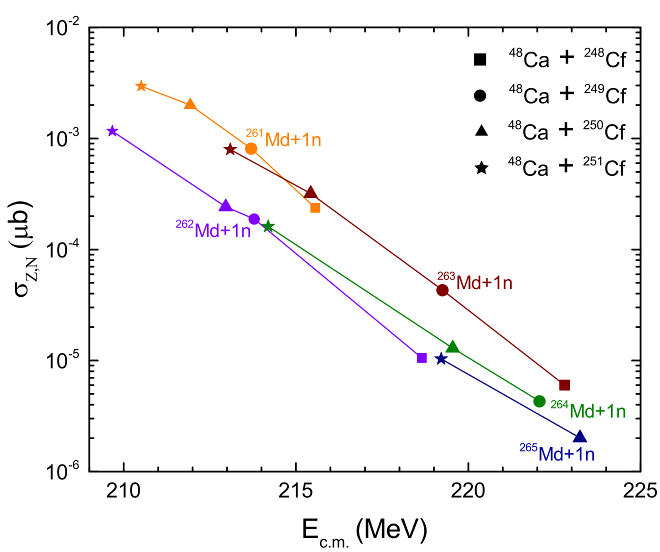

FIG. 4. The same as in Fig. 3 but in the $1n$ evaporation channel.

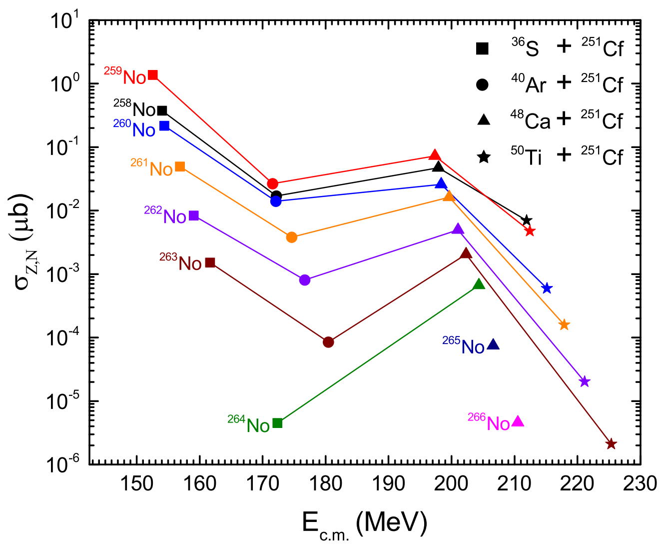

FIG. 5. The production cross sections of neutron-rich isotopes $^{258-266}$No calculated in the $0n$ evaporation channel as a function of incident energy $E_{\mathrm{c.m.}}$. Following multinucleon transfer, reactions are calculated: $^{36}\mathrm{S}+{}^{251}\mathrm{Cf}$ (squares), $^{40}\mathrm{Ar}+{}^{251}\mathrm{Cf}$ (circles), $^{48}\mathrm{Ca}+{}^{251}\mathrm{Cf}$ (triangles), and $^{50}\mathrm{Ti}+{}^{251}\mathrm{Cf}$ (stars). Lines with the same colors are drawn to trace the results for the same isotope of No.

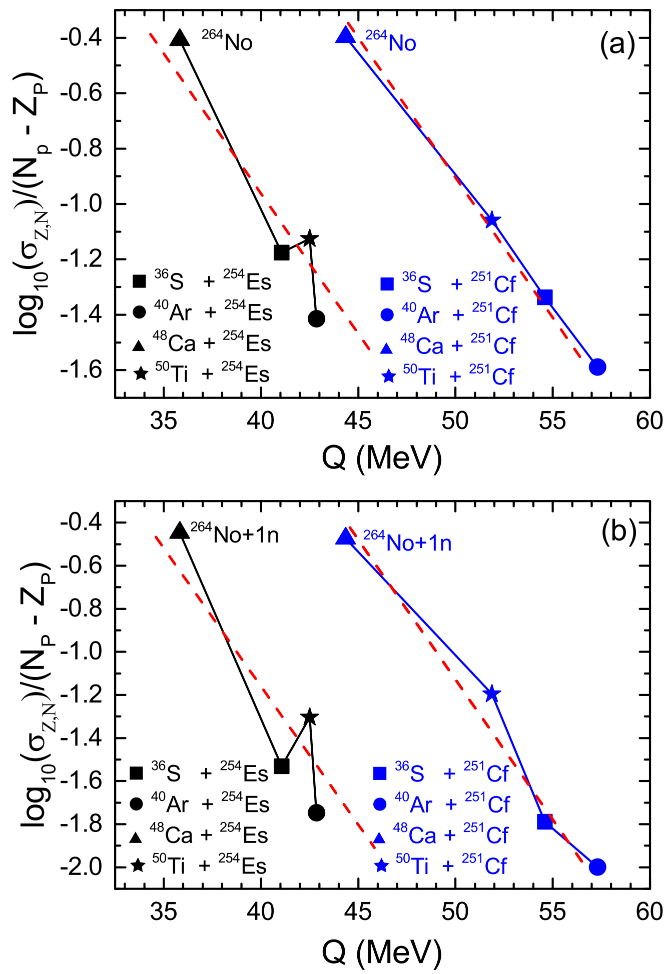

FIG. 6. The predicted values of $\log_{10}\sigma_{Z,N}/(N_P-Z_P)$ for ^{264}No as a function of Q. Panels (a) and (b) show the results in the $0n$ and $1n$ evaporation channels, respectively. The solid lines connect the results of different projectiles but obtained for the same target nucleus. The red dashed lines correspond to $k\approx 0.1$ in Eq. (2).

diffusion which occur between the two nuclei of the DNS. As a result of the nucleon transfer, it is possible to form the DNS configuration containing the heavy nucleus (Z,N) of interest which is defined here by the charge Z and neutron N numbers. This excited DNS can decay into two fragments and produce the primary yield of the reaction products in a search. After the decay, the primary fragments are mainly deexcited by neutron and γ emissions or go to fission channels.

Following the description of the DNS model, the production cross sections of certain nuclei are calculated as a three-step process. First, the initial DNS with the nucleus $(Z^{(i)},N^{(i)})$ is formed in the entrance reaction channel. Second, a new DNS configuration that contains an exotic nucleus (Z,N) is created through nucleon transfers. Finally, this DNS decays into two fragments and produces the exotic nucleus (Z,N) which is deexcited by emitting neutrons or γ rays. The production cross section in the three-step process is, thus, written as follows:

$$\sigma_{Z,N-x}=\sigma_{\mathrm{cap}}Y_{Z,N}W_{\mathrm{sur}}^{xn}, \tag{1}$$

where σ_{cap}, $Y_{Z,N}$, and W_{sur}^{xn} are the capture cross section to form a DNS from two reacting nuclei, the formation-decay probability of the DNS configuration with the given charge and mass asymmetries, and the survival probability of the excited exotic neutron-rich nucleus (Z,N) in the xn evaporation channel ($x=0$–2, ..., is the number of the emitted neutrons), respectively. In excited heavy nuclei, the neutron emission competes with fission. Because the same DNS model as in Ref. [36] is used here, we refer to Ref. [36] for the details of the calculations. Note that, for the calculation of $Y_{Z,N}$, we use the phase-space method (see Eq. (2) in Ref. [36]) which results in the upper limit of the estimated cross section. As in Refs. [27,28,49,50], this expression takes into account the stage of the N/Z equilibrium in the initial DNS.

As shown in Ref. [50], the statistical method results in almost the same yields as the dynamical calculations with the master equation in the reactions of interest. Although the yields of nuclei not far from the line of stability were treated in Ref. [50], there is no limitation for our statistical method to be applied for describing the yields of neutron-rich isotopes. The method was tested for the available experimental data in Refs. [28,49]. The interval of angular momentum was taken in accordance with the experimental conditions. The main condition of validity of our calculations is the formation of the DNS living longer than (3–5) $\times 10^{-21}$ s. At this interaction time, one can assume the statistic equilibrium in mass (charge) asymmetry coordinate.

III. CALCULATED RESULTS

In order to produce the neutron-rich isotopes of No ($^{258-266}$No), we consider the same multinucleon transfer

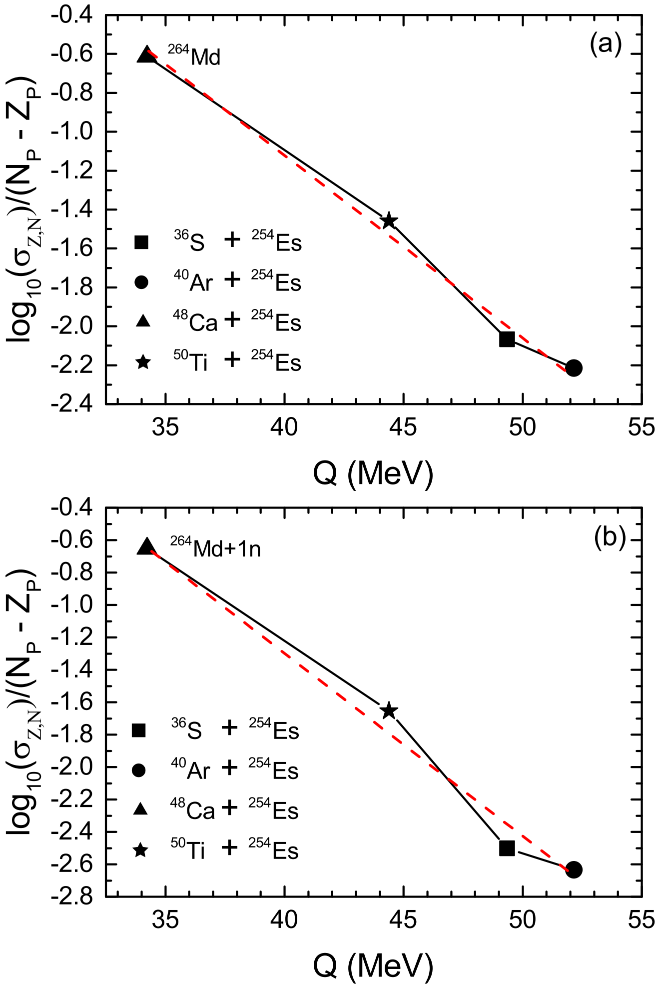

FIG. 7. The same as in Fig. 6 but for the production of ^{264}Md.

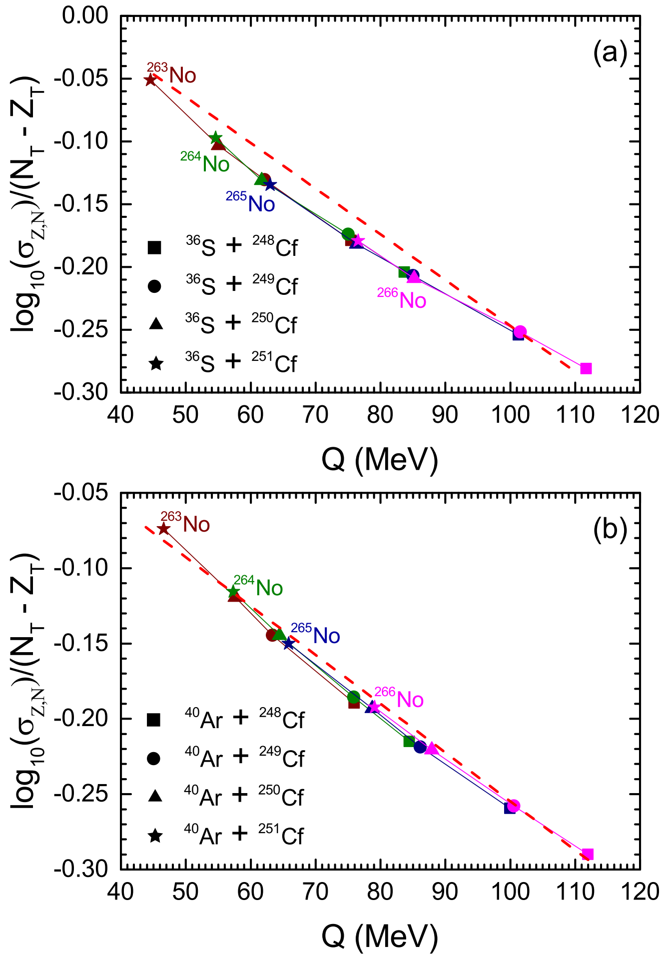

FIG. 8. The predicted values of $\log_{10} \sigma_{Z,N}/(N_T - Z_T)$ for $^{263-266}$No as a function of Q. The following reactions are calculated in the $0n$ evaporation channel: (a) ^{36}S + $^{248-251}$Cf and (b) ^{40}Ar + $^{248-251}$Cf. The solid lines of the same colors connect the results obtained for the same isotope.

reactions ^{36}S, ^{40}Ar, ^{48}Ca, ^{50}Ti + ^{254}Es, and $^{248-251}$Cf which were explored for the production of neutron-rich Md isotopes in our previous study [36]. As in the previous study, the reactions with ^{254}Es are expected to have the largest yields of $^{258-266}$No in the following schemes of their production: $^{36}\mathrm{S} + {}^{254}\mathrm{Es} \rightarrow {}^{40}\mathrm{S} + {}^{250}\mathrm{Es} \rightarrow {}^{32-26}\mathrm{Al} + {}^{258-264}\mathrm{No}$, $^{40}\mathrm{Ar} + {}^{254}\mathrm{Es} \rightarrow {}^{46}\mathrm{Ar} + {}^{248}\mathrm{Es} \rightarrow {}^{36-30}\mathrm{P} + {}^{258-264}\mathrm{No}$, $^{48}\mathrm{Ca} + {}^{254}\mathrm{Es} \rightarrow {}^{50}\mathrm{Ca} + {}^{252}\mathrm{Es} \rightarrow {}^{44-36}\mathrm{Cl} + {}^{258-266}\mathrm{No}$, and $^{50}\mathrm{Ti} + {}^{254}\mathrm{Es} \rightarrow {}^{54}\mathrm{Ti} + {}^{250}\mathrm{Es} \rightarrow {}^{46-41}\mathrm{K} + {}^{258-263}\mathrm{No}$. The calculations of $\sigma_{Z,N}$ with the $^{248-251}$Cf targets are performed similarly for the production of isotopes of interest. As seen, the calculation scheme takes into account the process of N/Z equilibrium in the initial DNS.

Figure 1 shows the predicted production cross sections of neutron-rich No isotopes in the $0n$ evaporation channel produced with the multinucleon transfer reactions considered in this paper. Throughout the paper, we present the cross sections larger than 1 pb only. The incident energy $E_{\mathrm{c.m.}}$ is chosen to make the excitation of the No isotope just below the corresponding neutron binding energy or fission barrier (more accurately, the smaller value of these two energies). Among all the reactions in consideration, the largest production cross sections of the heaviest isotopes $^{258-264}$No result from the ^{48}Ca + ^{254}Es reaction, although the ^{36}S + ^{251}Cf reaction has relatively large production cross sections. Note that, among the neutron-rich isotopes of No in consideration, isotopes up to ^{262}No ($\sigma_{Z,N} \approx 2$ nb) have been found experimentally to date. Also note that the ^{48}Ca + ^{254}Es reaction seems favorable for producing more exotic isotopes, such as $^{263-266}$No with the cross sections of 774, 263, 13, and 1 pb, respectively. The most neutron-rich No isotopes, ^{265,266}No, can be produced only in the ^{48}Ca + ^{254}Es reaction with cross sections larger than 1 pb.

If the beam energies were higher than those in Fig. 1, the evaporation processes are likely to occur in the primary excited products, and as a result, the reaction products of interest could be easily lost due to fission (in the neutron-rich isotopes of No considered in the heights of the fission barriers are smaller than the neutron separation energies). In this case, we have to take into account the one-neutron ($1n$) evaporation channel which competes with fission. In order to obtain the largest production cross section $\sigma_{Z,N}$ in the one-neutron evaporation channel, the value of incident

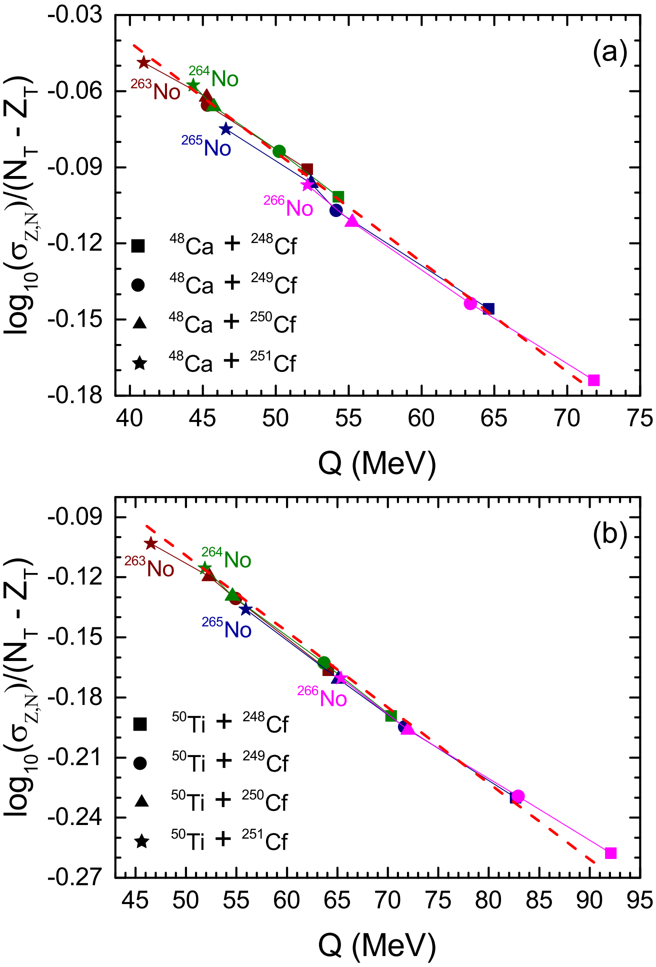

FIG. 9. The same as in Fig. 8 but for the reactions (a) $^{48}\mathrm{Ca} + {}^{248-251}\mathrm{Cf}$ and (b) $^{50}\mathrm{Ti} + {}^{248-251}\mathrm{Cf}$.

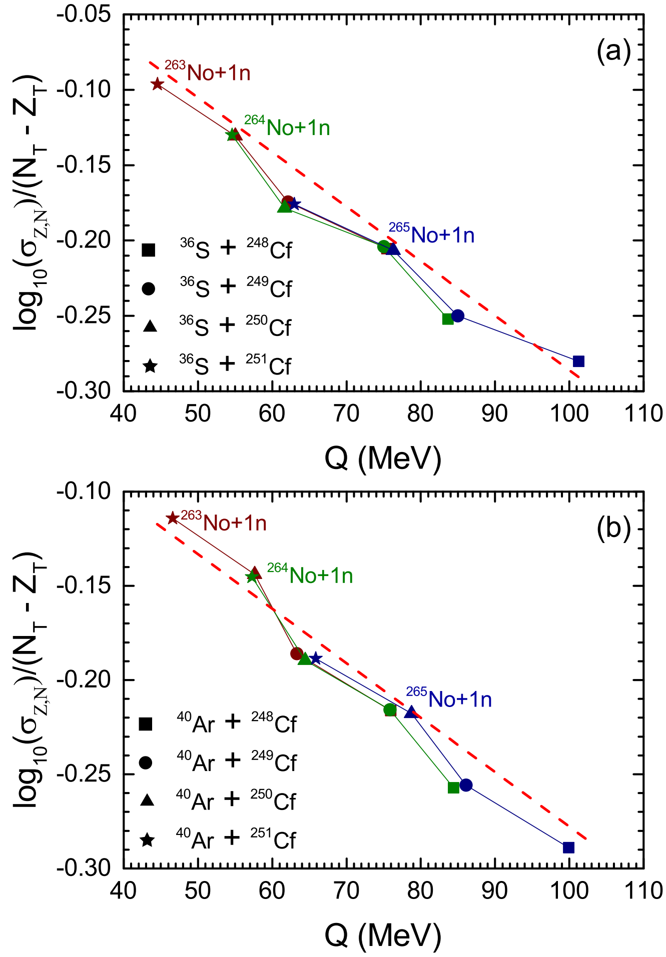

FIG. 10. The same as in Fig. 8 but for the $1n$ evaporation channel.

energy $E_{\mathrm{c.m.}}$ must correspond to the maximum of the excitation function. The calculated production cross sections of $^{258-266}$No in the $1n$ evaporation channel are presented in Fig. 2. The results obtained with the $1n$ evaporation channel show a similar trend to those with the $0n$ channel shown in Fig. 1; the largest production cross sections are from the $^{48}\mathrm{Ca} + {}^{254}\mathrm{Es}$ reaction. As seen, the predicted production cross sections for $^{258-260}$No are larger than 10 nb in the $^{48}\mathrm{Ca} + {}^{254}\mathrm{Es}$ reaction and several times larger than those in the $^{36}\mathrm{S} + {}^{254}\mathrm{Es}$ reaction. Our calculations show that the $^{48}\mathrm{Ca} + {}^{254}\mathrm{Es}$ reaction is the best way to produce the heaviest known isotope ^{262}No with $\sigma_{Z,N} \approx 2$ nb. The production cross sections of the presently unknown neutron-rich isotopes $^{263-266}$No are predicted as 744, 263, 13, and 1 pb, respectively.

In the $^{48}\mathrm{Ca} + {}^{254}\mathrm{Es}$ reaction, the DNS consisting of odd-even ^{43}Cl and ^{259}No has a lower potential energy than the DNS with odd-odd ^{42}Cl (^{260}No) or ^{44}Cl (^{258}No). As a result, ^{259}No is produced with a larger cross section than ^{258,260}No (see Fig. 1). In the case of the $1n$ evaporation channel of the same $^{48}\mathrm{Ca} + {}^{254}\mathrm{Es}$ reaction, the primary ^{259}No is also produced with the largest cross sections due to the reason mentioned above. However, after $1n$ evaporation occurs, the yield of ^{258}No becomes larger than those of ^{259,260}No (see Fig. 2). Comparison of Figs. 1 and 2 reveals that the production yields of neutron-rich No isotopes in the $0n$ evaporation channel are about several times larger than those in the $1n$ evaporation channel regardless of the reactions in consideration. This implies that uncertainties in the beam energy and target thickness do not affect the yields of the No isotopes of interest crucially as long as those uncertainties are within reasonable ranges.

Now, we present the results obtained with $^{248-251}$Cf as targets. Based on the results of our previous calculations on the Md isotopes in Ref. [36], the largest yields of neutron-rich No isotopes are expected in the reactions of ^{48}Ca with ^{251}Cf. Using the beam of ^{48}Ca, neutron-rich isotopes, $^{261-266}$No can be produced both in the $0n$ and in the $1n$ evaporation channels of the $^{48}\mathrm{Ca} + {}^{248-251}\mathrm{Cf}$ reactions (Figs. 3 and 4). Note that the production cross sections obtained with the $^{248-251}$Cf targets (shown in these two figures) are close to those with the ^{254}Es target (presented in Figs. 1 and 2). As shown in Figs. 3 and 4, the $^{48}\mathrm{Ca} + {}^{251}\mathrm{Cf}$ reaction seems most suitable to produce $^{263-266}$No with production cross sections of 2 nb (790 pb), 670 pb (160 pb), 75 pb (10 pb), and 5 pb, respectively, in the $0n$ ($1n$) channel. Similar to the ^{254}Es target, the production cross sections in the $0n$ evaporation channel are larger than those in the $1n$ evaporation channel. Because the ^{251}Cf target has the largest production cross section with the ^{48}Ca beam, it

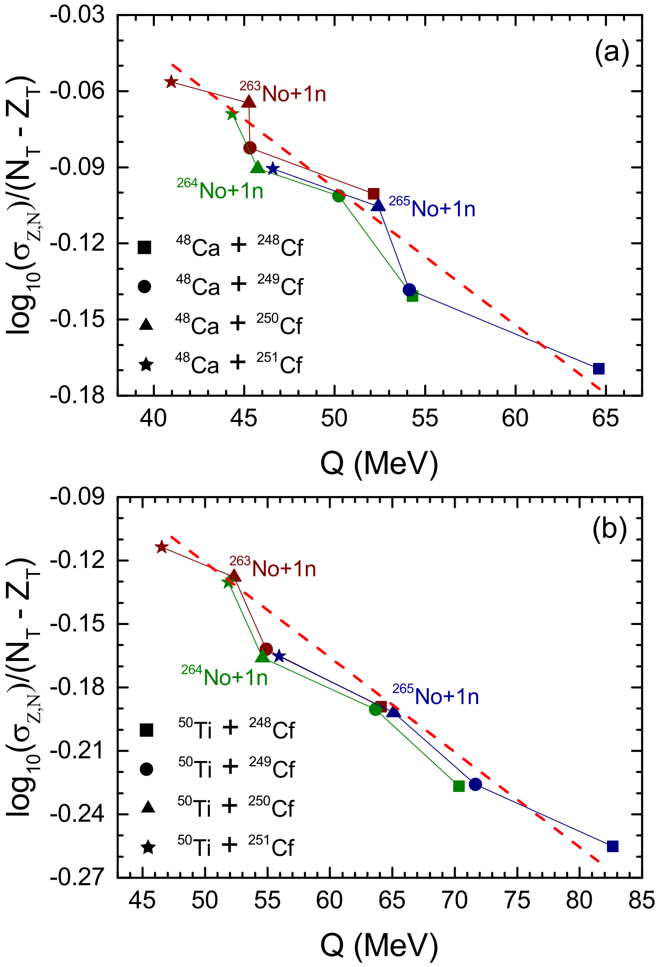

FIG. 11. The same as in Fig. 9 but for the $1n$ evaporation channel.

is worth calculating production cross sections with the other beams. Figure 5 shows these results. The predicted production cross sections of $^{258-266}$No are presented with the beam of ^{36}S, ^{40}Ar, ^{48}Ca, ^{50}Ti, and the ^{251}Cf target in the $0n$ channel. It is interesting that the $^{48}\mathrm{Ca}+{}^{251}\mathrm{Cf}$ reaction has larger production cross sections for neutron-rich isotopes $^{263-266}$No whereas the lighter isotopes are produced in the $^{36}\mathrm{S}+{}^{251}\mathrm{Cf}$ reaction with larger cross sections. Note that the trend of the production cross sections of neutron-richer isotopes $^{263-266}$No with the ^{251}Cf target resembles that with the ^{254}Es target, i.e., the reactions with the ^{48}Ca beam have the largest production cross sections (compare Figs. 1 and 5). This trend could be explained with similar charge asymmetries in two reactions. For example, in the case of ^{264}No, the charge asymmetries of the initial DNSs in both reactions [$\eta_Z(\mathrm{Ca}+\mathrm{Es}) = 0.664$ and $\eta_Z(\mathrm{Ca}+\mathrm{Cf}) = 0.661$] are close to those of the DNSs in the exit channels that contain ^{264}No ($\eta_Z = 0.714$ and 0.729, respectively).

Finally, we turn to the general trends in the production cross sections which depend on isospins of projectiles (P) or targets (T) and the Q values. First, we fix the target and consider the variations of the projectiles. As shown in Figs. 1 and 5, the reactions with the ^{36}S projectile have larger production cross sections by about an order of magnitude than those with the ^{40}Ar projectile regardless of the target, i.e., either ^{254}Es or ^{251}Cf. Note that isospin $N_P - Z_P = 4$ in both ^{36}S and ^{40}Ar, but in the reactions with ^{40}Ar, the Coulomb repulsion is stronger and, thus, the Q values for the formation of neutron-rich No isotopes are larger than in the reactions with ^{36}S. In the reactions with the ^{48}Ca projectile, the Coulomb repulsion is even larger, but larger isospin $N_P - Z_P = 8$ of this projectile reduces the Q values for the formation of neutron-rich isotopes and pushes the cross sections up in the end. Based upon the arguments above, we suggest that, in the reactions with fixed targets, the production cross sections of neutron-rich isotopes with $N - Z \geqslant 59$ can be roughly estimated with the following expression:

$$\log_{10} \sigma_{Z,N} \approx -k(N_P - Z_P)Q. \tag{2}$$

The coefficient k can be found by using the predicted production cross sections. For example, we present the current results for ^{264}No (Fig. 6) together with the previous ones for ^{264}Md (Fig. 7). In both cases, $k \approx 0.1$ regardless of the difference in the neutron evaporation ($0n$ or $1n$) channel. Note that we calculate all the values of Q in this paper by using the mass excesses from Refs. [51,52].

Now, we fix the projectile and vary the neutron number in the targets. In this case, we additionally fix the charge number (Z_T) of the given target nucleus. Similar to the projectile cases, we find that the production cross sections ($\log_{10} \sigma_{Z,N}$) depend on ($N_T - Z_T$) and Q as follows:

$$\log_{10} \sigma_{Z,N} \approx -k'(N_T - Z_T)Q. \tag{3}$$

Again, the coefficient k' can be found by using the predicted production cross sections. Figures 8 and 9 show the results with four different Cf targets $^{248-251}$Cf in the $0n$ channel. Even with different projectiles (^{36}S, ^{40}Ar, ^{48}Ca, and ^{50}Ti), almost the same value of $k' \approx 0.0035$ can fit the slopes in all four panels. Unlike in the projectile case, a slightly larger value of $k' \approx 0.004$ fits the slopes in the $1n$ evaporation channel as shown in Figs. 10 and 11. The previous results obtained for the neutron-rich isotopes of Md [36] are plotted in Fig. 12. The same value of $k' \approx 0.0035$ or 0.004 can fit the slope in the $0n$ (upper panel) or $1n$ (lower panel) channel. To calculate the cross sections shown in Figs. 3 and 4, we choose the optimal values of $E_{\mathrm{c.m.}}$ exceeding the corresponding Q value by a certain amount. Therefore, the plots in these figures are similar to those in Figs. 8–12. If we make a plot for the isotopic chain of No or Md for any reaction shown in Figs. 6 and 7, it would be similar to those presented in Figs. 8–12.

Equation (2) allows us to estimate the production cross sections in the reactions with a fixed target. So, it indicates the optimal projectile for the production of a certain isotope, whereas Eq. (3) indicates the optimal target at a given projectile. These two expressions are clearly based on the idea of the Q_{gg} systematics which is the main characteristic of the multinucleon transfer reactions [1]. Because the smaller the

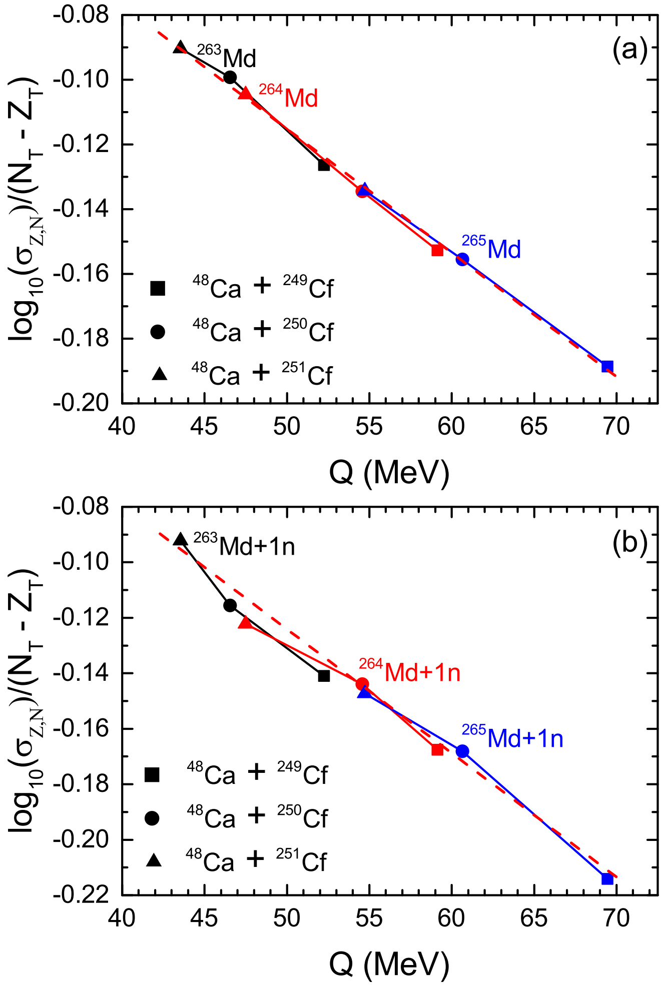

FIG. 12. The predicted values of $\log_{10}\sigma_{Z,N}/(N_T - Z_T)$ for $^{263-265}$Md as a function of Q obtained in our previous study. The $^{48}Ca + ^{249-251}Cf$ multinucleon transfer reactions are calculated in the (a) $0n$ and (b) $1n$ channels. The solid lines of the same colors connect the results for the same isotope.

Q value the larger the cross section, the physical meaning of Eqs. (2) and (3) becomes clear. However, the change of the DNS potential energy with respect to the initial DNS is defined not only by the change of Q value, but also by the change of the nucleus-nucleus interaction. For example, the Coulomb interaction changes with the DNS charge asymmetry. So, the coefficients k and k' together with the factors $(N_P - Z_P)$ and $(N_T - Z_T)$ take effectively into account the deviation of the Q value from the change of the DNS potential energy and the effect of DNS decay in R or toward more asymmetric and symmetric configurations.

IV. SUMMARY

Our current paper shows that the same reactions explored for the production of neutron-rich isotopes of Md in Ref. [36] are also good for producing neutron-rich isotopes of No, such as $^{263-266}$No with the production cross sections larger than ≈ 5 pb. However, the production cross sections for the neutron-rich isotopes of No are more than ten times smaller than those of Md. We find that, in transfer reactions, neutron-rich isotopes of heavy nuclei could be produced with larger cross sections if the charge asymmetry coordinates of the initial DNS were closer to those of the DNS in the exit channel that contains the nucleus of interest. By combining the current (No) and previous (Md) results, we suggest simple expressions for production cross sections of neutron-rich isotopes of the heavy nucleus in the transfer reactions. The logarithm of the production cross section is proportional to the isospin of the projectile or target and the Q value; see Eqs. (2) and (3).

ACKNOWLEDGMENTS

The work of M.-H.M. was supported by the Korea Institute of Science and Technology Information (KISTI). K.K. was also partly supported by the Basic Science Research Program through the National Research Foundation of Korea (Grant No. 2016R1A5A1013277). This work was also supported by RFBR (Grant No. 17-52-12015) and the DFG. The work of N.V.A. was supported by Tomsk Polytechnic University Competitiveness Enhancement Program grant.

[1] V. V. Volkov, Phys. Rep. **44**, 93 (1978).
[2] V. V. Volkov, in *Treatise on Heavy-Ion Science*, edited by D. A. Bromley (Plenum, New York, 1989), Vol. 8, Chap. 2, pp. 101–203.
[3] W. U. Schröder and J. R. Huizenga, in *Treatise on Heavy-Ion Science*, edited by D. A. Bromley (Plenum, New York, 1985), Vol. 2, pp. 113–726.
[4] M. Schädel *et al.*, Phys. Rev. Lett. **48**, 852 (1982).
[5] H. H. Freiesleben and J. V. Kratz, Phys. Rep. **106**, 1 (1984).
[6] H. Gäggeler *et al.*, Phys. Rev. C **33**, 1983 (1986).
[7] C. Y. Wu, X. T. Liu, S. P. Sorensen, R. W. Kincaid, M. W. Guidry, D. Cline, W. J. Kernan, E. Vogt, T. Czosnyka, A. E. Kavka, M. A. Stoyer, J. O. Rasmussen, and M. L. Halbert, Phys. Lett. B **188**, 25 (1987).
[8] C. Y. Wu, W. von Oertzen, D. Cline, and M. W. Guidry, Ann. Rev. Nucl. Part. Sci. **40**, 285 (1990).
[9] R. Broda, M. A. Quader, P. J. Daly, R. V. F. Janssens, T. L. Khoo, W. Ma, and M. W. Drigert, Phys. Lett. B **251**, 245 (1990).
[10] A. Türler *et al.*, Phys. Rev. C **46**, 1364 (1992).
[11] G. G. Adamian, A. K. Nasirov, N. V. Antonenko, and R. V. Jolos, Phys. Part. Nucl. **25**, 583 (1994).
[12] W. von Oertzen and A. Vitturi, Rep. Prog. Phys. **64**, 1247 (2001).
[13] B. Fornal *et al.*, Phys. Rev. C **70**, 064304 (2004).
[14] M. Rejmund, S. Bhattacharyya, A. Navin, W. Mittig, L. Gaudefroy, M. Gelin, G. Mukherjee, F. Rejmund, P. Roussel-Chomaz, and C. Theisen, Phys. Rev. C **76**, 021304(R) (2007).
[15] L. Corradi, G. Pollarolo, and S. Szilner, J. Phys. G: Nucl. Part. Phys. **36**, 113101 (2009).

[16] S. Lunardi, in *Perspective in Nuclear Physics: Proceedings of the 6th Japan-Italy Symposium on Heavy-Ion Physics*, edited by S.-C. Jeong, Y. Utsuno, T. Motobayashi, and A. Bracco, AIP Conf. Proc. No. 1120 (AIP, New York, 2009), p. 70.
[17] W. Królas, R. Broda, B. Fornal, T. Pawłat, J. Wrzesiński, D. Bazzacco, G. de Angelis, S. Lunardi, R. Menegazzo, D. R. Napoli, and C. Rossi Alvarez, Nucl. Phys. **A832**, 170 (2010).
[18] S. Heinz, V. Comas, S. Hofmann, D. Ackermann, J. Heredia, F. P. Hessberger, J. Khuyagbaatar, B. Kindler, B. Lommel, and R. Mann, Eur. Phys. J. A **43**, 181 (2010).
[19] W. Loveland, A. M. Vinodkumar, D. Peterson, and J. P. Greene, Phys. Rev. C **83**, 044610 (2011).
[20] S. A. Kalandarov, G. G. Adamian, and N. V. Antonenko, Phys. Part. Nucl. **43**, 825 (2012).
[21] V. Comas, S. Heinz, S. Hofmann, D. Ackermann, J. Heredia, F. P. Hessberger, J. Khuyagbaatar, B. Kindler, B. Lommel, and R. Mann, Eur. Phys. J. A **48**, 180 (2012).
[22] V. F. Comas, S. Heinz, S. Hofmann, D. Ackermann, J. Heredia, F. P. Hessberger, J. Khuyagbaatar, B. Kindler, B. Lommel, and R. Mann, Eur. Phys. J. A **49**, 112 (2013).
[23] E. M. Kozulin *et al.*, Phys. Rev. C **89**, 014614 (2014).
[24] H. M. Devaraja, S. Heinz *et al.*, Phys. Lett. B **748**, 199 (2015).
[25] S. Heinz *et al.*, Eur. Phys. J. A **52**, 278 (2016); G. G. Adamian, N. V. Antonenko, A. Diaz-Torres, and S. Heinz, *ibid.* **56**, 47 (2020).
[26] I. Stefan *et al.*, Phys. Lett. B **779**, 456 (2018).
[27] Yu. E. Penionzhkevich, G. G. Adamian, and N. V. Antonenko, Phys. Lett. B **621**, 119 (2005).
[28] Yu. E. Penionzhkevich, G. G. Adamian, and N. V. Antonenko, Eur. Phys. J. A **27**, 187 (2006).
[29] A. V. Karpov and V. V. Saiko, Phys. Rev. C **96**, 024618 (2017).
[30] V. V. Saiko and A. V. Karpov, Phys. Rev. C **99**, 014613 (2019).
[31] V. V. Saiko and A. V. Karpov, Acta Phys. Pol., B **50**, 495 (2019).
[32] V. I. Zagrebaev and W. Greiner, Phys. Rev. C **83**, 044618 (2011).
[33] V. I. Zagrebaev and W. Greiner, Phys. Rev. C **87**, 034608 (2013).
[34] M.-H. Mun, G. G. Adamian, N. V. Antonenko, Y. Oh, and Y. Kim, Phys. Rev. C **89**, 034622 (2014).
[35] M.-H. Mun, G. G. Adamian, N. V. Antonenko, Y. Oh, and Y. Kim, Phys. Rev. C **91**, 054610 (2015).
[36] M.-H. Mun, K. Kwak, G. G. Adamian, and N. V. Antonenko, Phys. Rev. C **99**, 054627 (2019).
[37] L. Zhu, Z.-Q. Feng, and F.-S. Zhang, J. Phys. G: Nucl. Part. Phys. **42**, 085102 (2015).
[38] Z.-Q. Feng, Phys. Rev. C **95**, 024615 (2017).
[39] L. Zhu, J. Su, W.-J. Xie, and F.-S. Zhang, Phys. Lett. B **767**, 437 (2017).
[40] P.-W. Wen, C. Li, L. Zhu, C.-J. Lin, and F.-S. Zhang, J. Phys. G: Nucl. Part. Phys. **44**, 115101 (2017).
[41] G. Zhang, C. Li, P.-W. Wen, J.-J. Li, X.-X. Xu, B. Li, Z. Liu, and F.-S. Zhang, Phys. Rev. C **98**, 014613 (2018).
[42] G. Zhang, C. A. T. Sokhna, Z. Liu, and F.-S. Zhang, Phys. Rev. C **100**, 024613 (2019).
[43] X. Bao, Nucl. Phys. A **986**, 60 (2019).
[44] A. Winther, Nucl. Phys. A **572**, 191 (1994).
[45] A. Winther, Nucl. Phys. A **594**, 203 (1995).
[46] A. Winther, GRAZING VERSION 9, http://personalpages.to.infn.it/~nanni/grazing/.
[47] S. Ayik, B. Yilmaz, O. Yilmaz, and A. S. Umar, Phys. Rev. C **100**, 014609 (2019).
[48] S. Ayik, B. Yilmaz, O. Yilmaz, and A. S. Umar, Phys. Rev. C **97**, 054618 (2018).
[49] G. G. Adamian, N. V. Antonenko, and D. Lacroix, Phys. Rev. C **82**, 064611 (2010).
[50] G. G. Adamian, N. V. Antonenko, and A. S. Zubov, Phys. Rev. C **71**, 034603 (2005).
[51] P. Möller, A. J. Sierk, T. Ichikawa, and H. Sagawa, At. Data Nucl. Data Tables **109**, 1 (2016); http://t2.lanl.gov/nis/data/astro/molnix96/molnix.html.
[52] M. Wang, G. Audi, F. G. Kondev, S. Naimi, and X. Xu, Chin. Phys. C **41**, 030003 (2017).